Constraining supersymmetry from the satellite experiments

Xiao-Jun Bi*

Key Laboratory of Particle Astrophysics, IHEP, Chinese Academy of Sciences, Beijing 100049, People's Republic of China

In this paper I study the detectability of γ rays from dark matter annihilation in the subhalos of the Milky Way by the satellite-based experiments EGRET and GLAST. I work in the frame of supersymmetric extension of the standard model and assume the lightest neutralino being the dark matter particles. Based on the N-body simulation of the evolution of dark matter subhalos I first calculate the average intensity distribution of this new class of γ-ray sources by neutralino annihilation. It is possible to detect these γ-ray sources by EGRET and GLAST. Conversely, if these sources are not detected the nature of the dark matter particles will be constrained by these experiments, depending, however, on the uncertainties of the subhalo profile.

I. INTRODUCTION

In the third EGRET catalog [1] unidentified γ-ray sources accounted for more than half of the discrete sources detected by EGRET. Despite a great effort, most of them cannot be associated with the known sources detected at low energies up to now. Most of the efforts in identifying these sources focused on the Galactic counterparts, such as young pulsars [2], microquasars [3], and supernova remnants [4]. At the same time, multiwavelength searches continue to look for counterparts in the γ-ray sources, such as blazars, supernova remnants, and pulsars [5]. There are recent theoretical works trying to explain the unidentified sources as annihilating dark matter clumps within the Milky Way (MW) [6]. These efforts try to solve the nature of dark matter.

The existence of cosmological dark matter has been firmly established by a multitude of observations, such as the observations of the rotation curves in spiral galaxies and velocity dispersion in elliptical galaxies, the x-ray emission and peculiar velocities of galaxies in the clusters of galaxies, the weak lensing effects, all indicating much steeper gravitational potentials than those inferred from the luminous matter. However, the nature of the nonbaryonic dark matter is still unknown and remains one of the most outstanding puzzles in particle physics and cosmology.

Among a large amount of theoretical candidates, the most attractive scenario involves the weakly interacting massive particles (WIMPs). An appealing idea is that the WIMPs form the thermal relics of the early Universe and naturally give rise to the relic abundance in the range of the observed values. The WIMPs are well motived theoretically by the physics beyond the standard model to solve the hierarchical problem between the weak scale and the Planck scale. In particular, the minimal supersymmetric extension of the standard model (MSSM) provides an excellent WIMP candidate as the lightest supersymmetric

particle (LSP), usually the lightest neutralino, which is stable due to R-parity conservation [7]. The cosmological constraints on the supersymmetric (SUSY) parameter space have been extensively studied in the literature [8].

The WIMPS can be detected on the present running or future experiments, either directly by measuring the recoil energy when a WIMP scatters off the detector nuclei [9] or indirectly by observing the annihilation products of the WIMPs, such as the antiprotons, positrons, γ rays, or neutrinos [10]. The rate of the WIMP annihilation is proportional to the number density squared of the dark matter particles. Therefore the searches for the annihilation signals should aim at the regions with high matter densities, such as at the Galactic center [11] or the nearby subhalos [12−14]. The existence of a wealth of subhalos throughout the Galaxy halos is a generic prediction of the cold dark matter paradigm of structure formation in the Universe. High resolution simulations show that for the cold dark matter scenario the large scale structure forms hierarchically by continuous merging of smaller halos and as the remnants of the merging process about 10% to 15% of the total mass of the halo is in the form of subhalos [15−22]. At the center of the subhalos there are high mass densities and therefore they provide good sites for the search of WIMP annihilation products.

However, the analysis in Refs. [6,23] shows that it seems most of the EGRET unidentified γ-ray sources are not produced by the dark matter annihilation. In [6] by comparing the cumulative luminosity function of subhalos and EGRET unidentified sources the authors found at most 26 ± 11 unidentified sources are possibly subhalos. However, location coincidence and variability cut even exclude further of these candidates [6]. In [23] assuming a similar population of subhalos between the Milky Way and M31 and using the upper limit of γ rays from M31 the authors found it is highly unlikely that a large fraction of these unidentified EGRET sources can be from subhalos. Improving the upper limit may finally exclude this possibility [23].

*bixj@mail.ihep.ac.cn

The strong constraints on the possible detectable subhalos from these works [6,23] will constrain the properties of dark matter particles. In the present work I assume that the neutralino forms dark matter and work in the frame of supersymmetric extension of the standard model. Assuming that none of the unidentified EGRET sources is from dark matter annihilation I will study how the properties of neutralino are constrained resorting to the numerical simulation result of dark matter clumps distribution. The nondetection of subhalos finally shows a constraint on the SUSY parameter space.

The next generation satellite-based experiment, GLAST [24], will greatly improve the sensitivity of EGRET. More γ-ray sources will be detected by GLAST. Detectability of γ rays from the subhalos by GLAST has been studied in the literature [13,25–31]. Once such sources are detected, the follow-up study of the sources may measure the spectrum of the annihilated γ- rays or even detect the line emission [31]. These measurements will finally give strong implications on the properties of dark matter. However, there are also possibilities of null results for such searches, similar to the EGRET result or the null result of direct detection even though the direct detection has continuously improved sensitivities. In this case I would like to study how supersymmetry would be constrained.

It is well known that the flux of gamma rays from the neutralino annihilation in a clump is given by

$$
\begin{aligned}
\Phi(E) &= \frac{\langle \sigma v \rangle}{2m^2} \frac{dN}{dE} \int dV \frac{\rho^2}{4\pi d^2} \\
&= \frac{1}{4\pi} \frac{\langle \sigma v \rangle}{2m^2} \frac{dN}{dE} \times \frac{1}{d^2} \int_0^{\bar{r}} 4\pi r^2 \rho^2(r) dr, \quad (1)
\end{aligned}
$$

where $\langle \sigma v \rangle$ is the annihilation cross section times the relative velocity, $\frac{dN}{dE}$ is the differential flux in a single annihilation, m is the mass of the dark matter particle, and d is the distance from the detector to the source. The flux depends on both the distribution of the dark matter $\rho(r)$ and the particle nature of dark matter.

In the next section I first give the intensity distribution of the subhalo γ-ray sources according to the N-body simulation results. Then in Sec. III I present the constraints on the SUSY parameter space from nondetection of the subhalo γ-ray sources by EGRET and GLAST. I finally give a conclusion in Sec. IV.

II. DISTRIBUTION OF SUBHALOS AND THEIR γ-RAY INTENSITIES

In this section I first present some simulation results about the subhalos and then I calculate the intensities of the MW subhalos as γ-ray sources by neutralino annihilation.

N-body simulations show that the radial distribution of substructures is generally shallower than the density profile of the smooth background due to the tidal disruption of

substructures which is most effective near the galactic center [32]. The relative number density of subhalos is approximately given by an isothermal profile with a core [32]

$$
n(r) = 2n_H (1 + (r/r_H)^2)^{-1}, \quad (2)
$$

where n_H is the relative number density at the scale radius r_H, with r_H being about 0.14 times the halo virial radius $r_H = 0.14 r_{\mathrm{vir}}$. The result given above agrees well with that in another recent simulation by Gao *et al.* [33].

The differential mass function of substructures has an approximate power-law distribution, $dn/dm \sim m^{-\alpha}$, with $\alpha = -1.7 \sim -2$ [32–34]. In Refs. [32,34] both the cluster and galaxy substructure cumulative mass functions are found to be an m^{-1} power law, $n_{\mathrm{sub}}(m_{\mathrm{sub}} > m) \propto m^{-1}$, with no dependence on the mass of the parent halo. A slight difference is found in a simulation by Gao *et al.* [33] that the cluster substructure is more abundant than the galaxy substructure since the cluster forms later and more substructures have survived the tidal disruption. The mass function for both scales are well fitted by $dn/dm \propto m^{-1.9}$. Taking the power index of the differential mass function greater than -2 makes the fraction of the total mass enclosed in subhalos insensitive to the mass of the minimal subhalo. The mass fraction of subhalos estimated in the literature is around between 5% to 20% [18,19,34,35]. In this work I will take the differential index of -1.9 and the mass fraction of substructures as 10%.

To calculate the γ-ray intensities from the dark matter clumps I first realize a MW-like halo with a population of subhalos due to the subhalo distribution function from simulation, which is given above. The masses of the substructures are taken randomly between $M_{\mathrm{min}} = 10^6 M_{\odot}$, which is the lowest substructure mass the present simulations can resolve [36], and the maximal mass M_{max}. The maximal mass of the substructures is taken to be $0.01 M_{\mathrm{vir}}$ since the MW halo does not show recent mergers of satellites with masses larger then $\sim 2 \times 10^{10} M_{\odot}$. The γ-ray flux is quite insensitive to the minimum subhalo mass since the flux from a single subhalo scales with its mass [13,34,37].

However, due to the finite spatial resolution of the N-body simulations the distribution in Eq. (2) is an extrapolation of the subhalo distribution at large radius. The formula underestimates of the tidal effect which destroys most substructures near the Galactic center (GC). I take the tidal effects into account under the "tidal approximation," which assumes that all mass beyond the tidal radius is lost in a single orbit while keep its density profile inside the tidal radius intact.

The tidal radius of the substructure is defined as the radius at which the tidal forces of the host exceed the self-gravity of the substructure. Assuming that both the host and the substructure gravitational potential are given by point masses and considering the centrifugal force

experienced by the substructure the tidal radius at the Jacobi limit is given by [38]

$$r_{\text{tid}} = r_c \left(\frac{m}{3M(r < r_c)} \right)^{(1/3)}, \qquad (3)$$

where r_c is the distance of the substructure to the GC, and $M(r < r_c)$ refers to the mass within r_c.

The substructures with $r_{\text{tid}} \lesssim r_s$ will be disrupted. The mass of a substructure is recalculated by subtracting the mass beyond the tidal radius in realizing the MW-like halos. After taking the tidal effects into account I find the substructures near the GC are disrupted completely.

A. Concentration parameter

I adopt both the Navarro, Frenk, and White (NFW) [39,40] and the Moore [41,42] profiles for the subhalos in my calculation, which can be written in a general form as

$$\rho = \frac{\rho_s}{(r/r_s)^\gamma [1 + (r/r_s)^\alpha]^{(\beta - \gamma)/\alpha}}, \qquad (4)$$

where ρ_s and r_s are the scale density and scale radius, respectively. $(\alpha, \beta, \gamma) = (1, 3, 1)$ and $(1.5, 3, 1.5)$ are for the NFW and Moore profiles, respectively.

The free parameters ρ_s and r_s can be determined by the mass and concentration parameter of the subhalo. The concentration parameter is defined as

$$c = \frac{r_{\text{vir}}}{r_{-2}}, \qquad (5)$$

where r_{vir} is the virial radius of the halo and r_{-2} is the radius at which the effective logarithmic slope of the profile is -2, i.e., $\frac{d}{dr}(r^2 \rho(r))|_{r=r_{-2}} = 0$. For the NFW profile I have $r_s = r_{-2}$, while for the Moore profile I have $r_s = r_{-2}/0.63$.

The concentration parameter is a crucial parameter in determining the γ-ray fluxes from subhalos. From the definition of the concentration parameter in Eq. (5) and the annihilation flux in Eq. (1) I can easily get that the annihilation flux from a clump is proportional to $\phi \sim A\rho_s^2 r_s^3 \sim A m_{\text{sub}} c^3$ with A a flat function of c. Therefore the annihilation flux is very sensitive to the concentration parameter. The concentration parameter is obtained by N-body simulations. However, due to the finite resolution of N-body simulations, numerical convergence has not been established, especially for the evolution of subhalos. Adopting different models the predicted detectable number of subhalos at GLAST (at 5σ for 1 yr exposure) spans from $\lesssim 1$ by Koushiappas et al. [13] to at most about 300 by Baltz et al. [31]. Recently Pieri et al. tried to classify different cases by modeling the subhalos concentration parameter and found the detectable number of subhalos at GLAST ranges from ~ 0 to ~ 40 [27] for different models they adopted. Another way for this kind of study

is directly based on the simulation result, such as in the recent work by Diemand et al. [34]. In this work I will adopt different analytic models or the fit formulas based on simulation results about subhalos in the literature to discuss their detectability. Uncertainties of the simulation results are thus included in my study.

I first introduce a semianalytic model to determine the concentration parameter given by Bullock et al. [43] which is built based on their simulation result. In the model, at an epoch of redshift z_c a typical collapsing mass $M_*(z_c)$ is defined by $\sigma[M_*(z)] = \delta_{sc}(z)$, where $\sigma[M_*(z)]$ is the linear rms density fluctuation on the comoving scale encompassing a mass M_*, and δ_{sc} is the critical overdensity for collapsing at the spherical collapse model. The model assumes the typical collapsing mass is related to a fixed fraction of the virial mass of a halo $M_*(z_c) = FM_{\text{vir}}$. The concentration parameter of a halo with virial mass M_{vir} at redshift z is then determined as $c_{\text{vir}}(M_{\text{vir}}, z) = K\frac{1+z_c}{1+z}$. Both F and K are constants to fit the numerical simulations. A smaller M_{vir} corresponds to a smaller collapsing mass and early collapsing epoch when the Universe is denser and therefore a larger concentration parameter. Figure 1 plots the concentration parameter at $z = 0$ as a function of the virial mass of a halo according to the Bullock model [43].

From Fig. 1 it can be seen that between the masses $10^6 M_\odot \sim 10^{10} M_\odot$ an experiential formula $c_{\text{vir}} \propto M_{\text{vir}}^{-\beta}$ reflects the simulation result accurately. I expect that this power-law relation should be very well followed, since subhalos form early at the epoch when the Universe is dominated by matter with an approximate power-law power spectrum of fluctuations [43].
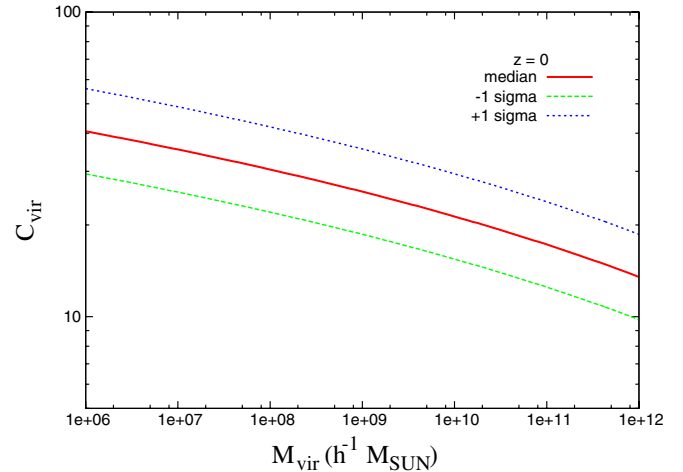

FIG. 1 (color online). Concentration parameter as a function of the virial mass calculated according to the Bullock model [43]. The model parameters are taken as $F = 0.015$ and $K = 4.4$. The cosmology parameters are taken as $\Omega_M = 0.3$, $\Omega_\Lambda = 0.7$, $\Omega_B h^2 = 0.02$, $h = 0.7$, and $\sigma_8 = 0.9$ with three generations of massless neutrinos and a standard scale invariant primordial spectrum. Both the median and the $\pm 1\sigma$ values of the concentration parameters are plotted.

In the literature another widely adopted semianalytical model for the concentration parameter is given by Eke, Navarro, and Steinmetz (ENS) [44]. I also adopt the ENS model for the ΛCDM model with $\sigma_8 = 0.9$. The other two models I adopted are the simulation results by Reed *et al.* [45] and that by Bullock for the subhalos in a dense environment [43]. I will show that these models predict very different annihilation fluxes. Especially for subhalos within the dense environment, the simulation indicates it may have greater concentration than those of isolated halos [43] and therefore lead to larger annihilation flux.

B. γ-ray intensity of the subhalos

Once the profile parameters of each subhalo are determined and, in each realization of the MW-like halos, the distribution of subhalos is also known, I can calculate the γ-ray fluxes from these subhalos. Then I can plot the number of sources as a function of their intensities. By realizing 100 such MW sized halos I give the averaged number of sources as a function of their intensities. I have fixed the property of the neutralino by requiring the γ-ray flux of 3.7×10^{-9} ph cm^{-2} s^{-1} sr^{-1} from the GC assuming a NFW profile. Fixing the flux from the GC actually gives the relative intensities between the GC and each subhalo.

Figure 2 gives the cumulative number of subhalos emitting γ rays with fluxes greater than a value Φ_γ. In the left panel I plot the results for the Moore profile while the right panel is for the NFW profile. From Fig. 2 I can easily read the expected number of detectable subhalos if the sensitivity of a detector is given with the same field of view. For example, the sensitivity of GLAST at 5σ for 1 yr exposure reaches 2×10^{-10} cm^{-2} s^{-1} sr^{-1} [46]. For comparison I

adopt the same particle factor as Pieri *et al.* [27], which is about 3 orders of magnitude larger than my particle factor adopted here and get the detectable subhalo number in the NFW profile from ~ 0 to ~ 400. The maximal detectable number of subhalos predicted by Pieri *et al.* [27] is only about 40, however, which is given in a different scenario from the "subhalo" case here. My result is consistent with the result by Baltz *et al.* [31]. Even for this scenario and with the optimistic particle factor I have only about 2 detectable subhalos at EGRET, whose 5σ sensitivity can only reach $\sim 10^{-8}$ cm^{-2} s^{-1}.

Figure 2 shows that there is a large discrepancy for predictions based on different models. Especially the "subhalo" model gives much greater prediction. The reason is directly related to the large concentration parameters for the subhalo scenario. It should be noted that the other three models actually describe distinct halos with small masses. A qualitative simulation result about the concentration parameter is that it is determined by the halo collapse time, as shown in the Bullock model. The reason of the large concentration parameter for subhalo is that in dense environment halos tend to collapse much earlier [43]. Tidal stripping may also lead to stronger mass dependence of concentration on the subhalo mass. Another reason is that a high density environment likely leads to extreme collapse histories of subhalos and frequent merger events which affect the final concentration (for more discussions see [43]).

C. Detector sensitivities

Before going on to the next section I first discuss the sensitivities of EGRET and GLAST. The detectability of a signal is defined by the ratio of the signal events to the
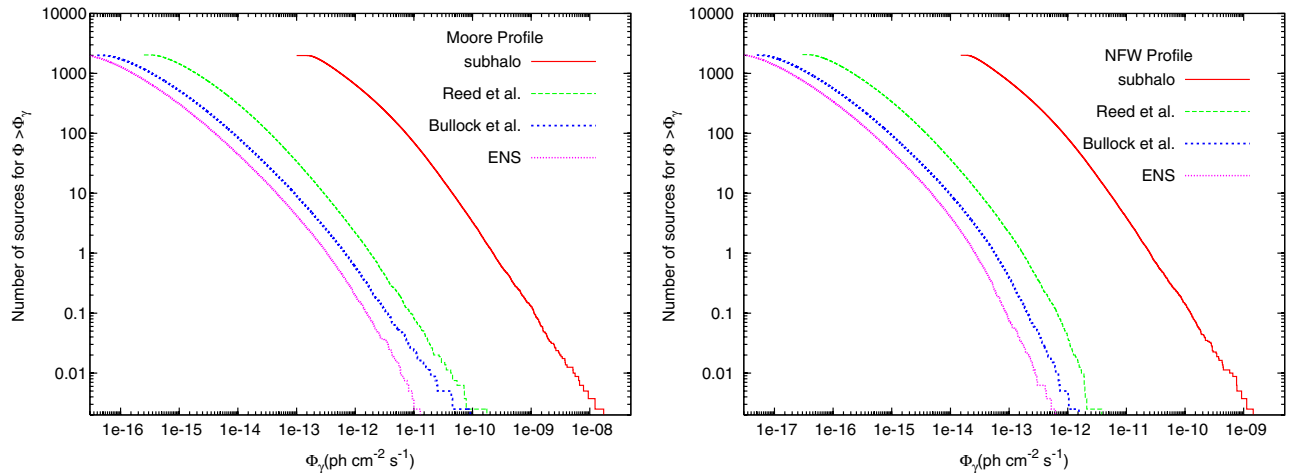

FIG. 2 (color online). The cumulative number of subhalos as a function of the integrated γ-ray fluxes $n(>\Phi_\gamma)$ for the Moore profile (left panel) and the NFW profile (right panel) within the solid angle of π. Subhalos are taken as point sources within the angular resolution of 1°. The curves are corresponding to different simulation results, where "subhalo" denotes the model for subhalos within a smooth halo [43]; "Reed *et al.*" refers to the simulation results given by Reed *et al.* in [45]; "Bullock *et al.*" uses the median $c_{\mathrm{vir}} - M_{\mathrm{vir}}$ relation for distinct halos of the Bullock model in [43]; "ENS" refers to the result of Eke *et al.* [44].

fluctuation of the background. Since the background follows the Poisson statistics, its fluctuation has an amplitude proportional to $\sqrt{N_B}$. The *significance* of the detection is quantified by $\sigma = \frac{n_\gamma}{\sqrt{N_B}}$.

The signal events are given by

$$n_\gamma = \epsilon_{\Delta\Omega} \int_{E_{\text{th}}, \Delta\Omega} A_{\text{eff}}(E, \theta)\phi(E)dEd\Omega dT, \qquad (6)$$

where $\epsilon_{\Delta\Omega} = 0.68$ is the fraction of signal events within the angular resolution of the instrument and the integration is for the energies above the threshold energy E_{th}, within the angular resolution of the instrument $\Delta\Omega$ and for the observational time. Generally the effective area A_{eff} is a function of energy and zenith angle. The $\phi(E)$ is the flux of γ rays from dark matter (DM) annihilation. I take $E_{\text{th}} =$ 1 GeV for both EGRET and GLAST. EGRET has angular resolution of $\sim 1°$ while GLAST has much better angular resolution of $\sim 0.1°$.

The corresponding expression for the background is similar to Eq. (6). Adopting the measured background flux $\phi^{BG}(E)$, which is expected to get much better precision by GLAST and PAMELA, and if one knows the effective area of the detectors and the identification efficiency for the charged particles (of hadronic and electronic background) and photons one can get the sensitivity of the detector [14]. The ''sensitivity'' means for some time exposure, for example, for 1 yr, the minimal flux the source has in order to have a 5σ detection.

The sensitivity is not difficult to estimate for EGRET and GLAST, as given in [14]. However, a careful simulation of the detector is beyond the present study. I will take the sensitivities of EGRET and GLAST directly from the literature [46], that is, 3×10^{-8} and 2×10^{-10} ph cm^{-2} s^{-1}, respectively. In [46] the sensitivities of EGRET and GLAST are for 1 yr of all sky survey with the diffuse gamma background from EGRET as 2×10^{-5} ph cm^{-2} s^{-1} sr^{-1}(100 MeV/E)$^{1.1}$, the typical background at high galactic latitudes. Considering background at different latitudes and longer observation time will certainly change the sensitivity. However, the exact values of the detector sensitivities are not very important, since the constraints on the SUSY parameter space given in the following can be simply rescaled with the sensitivity. From Fig. 2 one can easily understand this: if sensitivity is lowered by a factor n the particle factor that can be probed is also lowered by the factor n.

For GLAST I have calculated a similar result to that in Fig. 2 with better angular resolution. For the Moore profile there is very small difference from Fig. 2, which means most annihilation takes place within the very innermost region at the halo center. For the NFW profile there are differences for the number of the brightest γ-ray sources, which may be from subhalos near the Sun. For these nearby sources different angular resolution leads to different γ-ray fluxes when taking the NFW profile.

III. CONSTRAINTS ON THE SUSY PARAMETERS

From the results in the last section I can predict the number of γ-ray sources detectable in EGRET or GLAST for any SUSY models. Conversely, if no source is detected the SUSY models are constrained.

I will work in the frame of MSSM, the low energy effective description of the fundamental theory at the electroweak scale. By doing a random scan I give how the parameter space is constrained by these detectors.

However, there are more than 100 free SUSY breaking parameters even for the R-parity conservative MSSM. A general practice in phenomenological studies is to assume some simple relations between the parameters and greatly reduce the number of free parameters. Following the assumptions in DarkSUSY [47] I take seven free parameters in calculating dark matter production and annihilation, i.e., the Higgsino mass parameter μ, the wino mass parameter M_2, the mass of the CP-odd Higgs boson m_A, the ratio of the Higgs vacuum expectation values $\tan\beta$, the scalar fermion mass parameter $m_{\tilde{f}}$, the trilinear soft-breaking parameter A_t and A_b. All the sfermions have taken a common soft-breaking mass parameter $m_{\tilde{f}}$; all trilinear parameters are zero except those of the third family; the bino and wino have the mass relation $M_1 = 5/3\tan^2\theta_W M_2$, coming from the unification of the gaugino mass at the grand unification scale. The simplification of the parameters actually does not decrease the generality of my discussion, since the seven parameters are the most relevant ones for the purpose. Including other parameters will not change my results much.

I perform a numerical random scan in the 7-dimensional supersymmetric parameter space using the package DarkSUSY [47]. The ranges of the parameters are as
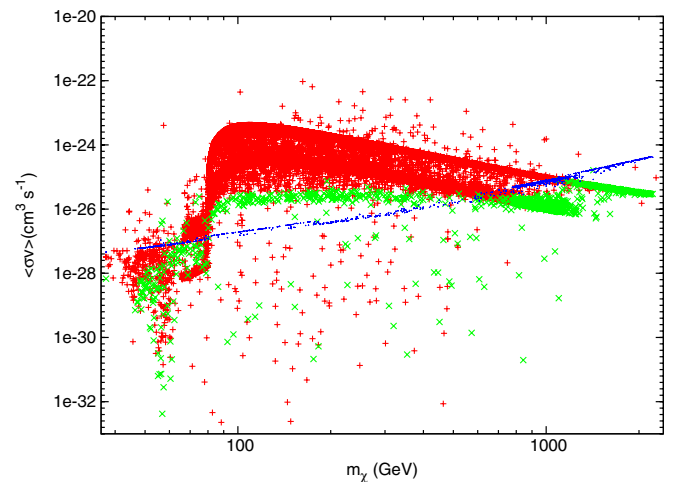

FIG. 3 (color online). The points in the figure represent models produced randomly in the SUSY parameter space. The narrow strip represents the critical values of $\langle\sigma v\rangle$ for these models, as explained in the text. In the following figures I use thick curves to represent the strip.
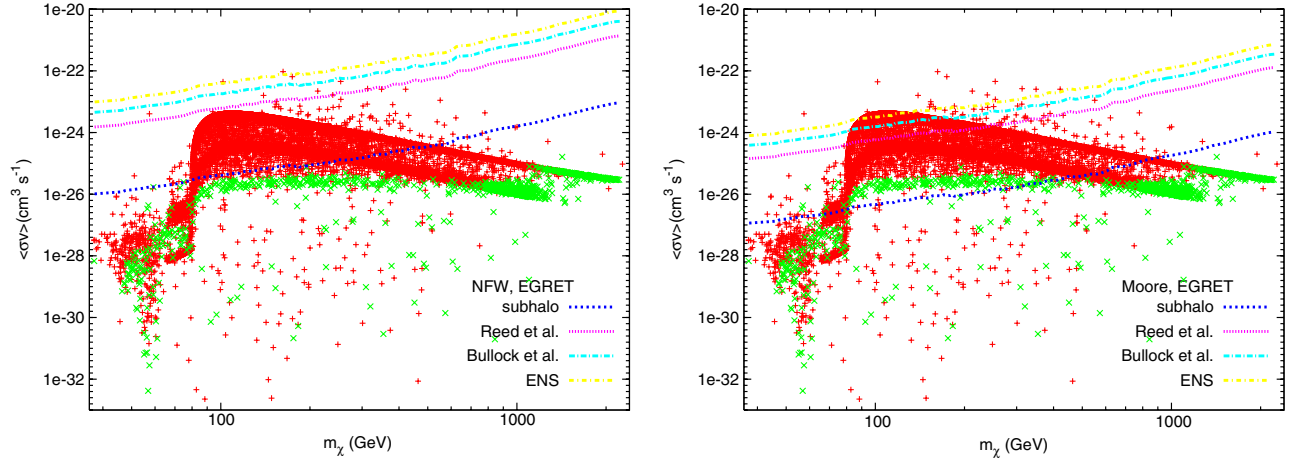
FIG. 4 (color online).   Constraints of EGRET on the SUSY parameter space if no γ-ray sources are detected at the 5σ level from dark matter clumps. The left panel gives the constraints assuming a NFW profile while the right is for a Moore profile. The points in the figure represent models produced randomly in the SUSY parameter space. Models above the curves are ruled out. Different curves are given adopting different simulation results, as explained in the text. The models which satisfy the relic density within 4σ (xes) have smaller $\langle\sigma v\rangle$ than these having $\Omega h^2 < 0.053$ (crosses).

following: 50 GeV $< |\mu|$, M_2, M_A, $m_{\tilde{f}} < 10$ TeV, $1.1 <$ $\tan\beta < 61$, $-3m_{\tilde{q}} < A_t$, $A_b < 3m_{\tilde{q}}$, $\text{sign}(\mu) = \pm 1$. The parameter space is constrained by the theoretical consistency requirement, such as the correct vacuum breaking pattern, the neutralino being the LSP and so on. The accelerator data constrains the parameter further from the spectrum requirement, the invisible Z-boson width, and the branching ratio of $b \rightarrow s\gamma$ [47].

The SUSY models are divided into two groups: those that satisfy the constraint of dark matter relic density within 4σ for $\Omega_\chi h^2 = 0.105^{+0.007}_{-0.013}$ [48] and those that do not satisfy, i.e., $\Omega_\chi h^2 < 0.053$. The effect of coannihilation between the fermions is taken into account when calculating the relic density numerically. For the second group of models I assume the neutralino is produced by some nonthermal mechanism [49] to satisfy the observation.

I then derive the constraints on the SUSY parameter space. Having known the sensitivities, according to the result in Fig. 2 I can get the detectable number of γ-ray sources in EGRET and GLAST for the SUSY model I took in the last section. When I scan in the SUSY parameter space, I calculate the average detectable number of subhalos at EGRET and GLAST for each SUSY model. Then I scale the value of $\langle\sigma v\rangle$ to a critical value that only one subhalo can be detected. The SUSY parameters with larger $\langle\sigma v\rangle$ than the critical value of $\langle\sigma v\rangle$ should be excluded by the experiments if null results are gotten. In Fig. 3 I show the critical values of $\langle\sigma v\rangle$ according to the procedure above, which form a narrow strip. I would expect that the constraints should be divergent since the annihilation final states should be very different. However, according to Fig. 3 I know that the γ-ray spectra from different final
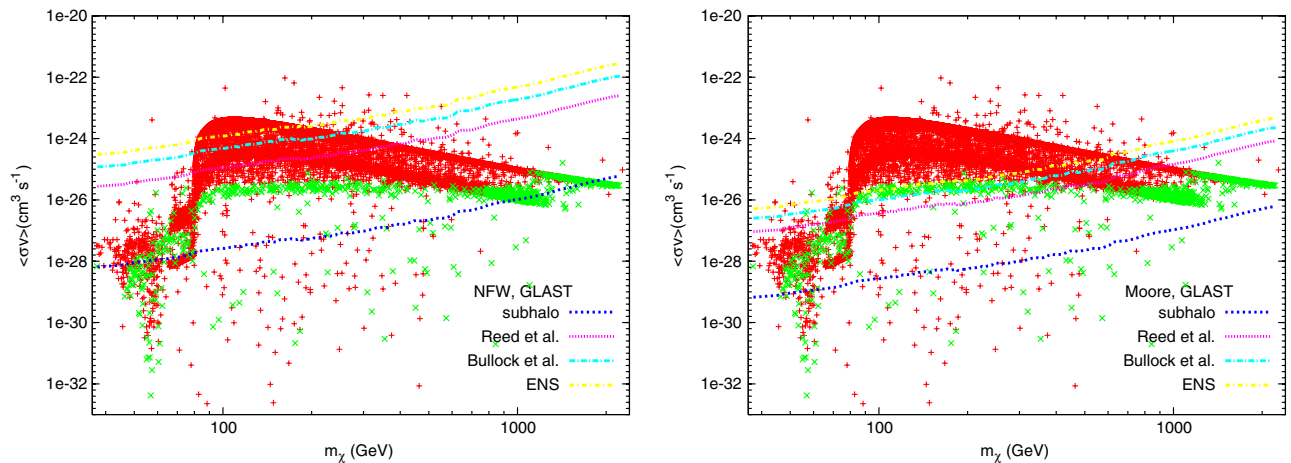

FIG. 5 (color online).   Same as Fig. 4 except that the constraints are from GLAST.

states with the same m_χ should be quite similar so that I get a convergent result. In the following figures I use thick curves to represent these strips.

In Fig. 4 I show the constraints of EGRET on the SUSY parameter space if no unidentified γ-ray sources are from dark matter clumps. The left panel gives the constraints assuming the NFW profile while the right is for the Moore profile. I notice for the NFW profile only the "subhalo" scenario can constrain the nonthermal SUSY models. For the Moore profile the subhalo scenario can also constrain a part of the thermal SUSY models. The other scenarios have quite weak constraints on the models by EGRET. For light neutralinos the constraints on $\langle \sigma v \rangle$ are 10^{-26} cm^{-3} s^{-1} and 10^{-27} cm^{-3} s^{-1} for the NFW and Moore profiles, respectively, in the subhalo scenario. For other models the constraints are $\sim 10^{-24}$ cm^{-3} s^{-1} and $\sim 10^{-25}$ cm^{-3} s^{-1} for NFW and Moore profiles, respectively. Notice that the models with $\Omega h^2 < 0.053$ have a greater $\langle \sigma v \rangle$ than those thermal models and therefore produce larger γ-ray fluxes. These models are easier to be ruled out.

In Fig. 5 I show the similar constraints on SUSY by GLAST, which can give much severer constraints on the parameter space than EGRET gives. For the Moore profile all scenarios can put constraints on the SUSY models. In this case a large fraction of the nonthermal parameter space will be ruled out. The constraints on $\langle \sigma v \rangle$ for light neutralinos are now 10^{-28} cm^{-3} s^{-1} and 10^{-29} cm^{-3} s^{-1} for the NFW and Moore profiles, respectively, in the "subhalo" scenario. For other models the constraints on $\langle \sigma v \rangle$ reach $\sim 10^{-26}$ cm^{-3} s^{-1} and $\sim 10^{-27}$ cm^{-3} s^{-1} for the NFW and Moore profiles, respectively.

IV. DISCUSSIONS AND CONCLUSION

Since the rate of dark matter annihilation is proportional to the DM density squared, the Galactic center had been considered as the most promising site to search for the annihilation signals. The possibility of detecting dark matter annihilation from the GC has been extensively studied in literature [11]. However, the GC is a very complex environment. The dark matter density profile near the GC is complicated due to the existence of baryonic matter and leads to difficulties in making theoretical calculations. For example, the supermassive black hole (SMBH) can either steepen or flatten the slope of the DM profile at the innermost center of the halo depending on the evolution of the black hole [50]. Furthermore, the baryonic processes associated with the central SMBH and the supernova remnant Sgr A* [51] provide a strong γ-ray background, which has been detected by HESS [52], to the signals of dark matter annihilation and make the detection very difficult [51]. In [51] it is found that in the case of the NFW profile GLAST can probe $\langle \sigma v \rangle$ between 10^{-26} cm^{-3} s^{-1} and 10^{-28} cm^{-3} s^{-1} for light neutralinos, which is similar to

the sensitivity by observing subhalos as shown in Fig. 5. However, considering the HESS detected γ-ray background, only models with $\langle \sigma v \rangle \gtrsim 10^{-27}$ cm^{-3} s^{-1} can be probed [51] from the GC by GLAST. Therefore it becomes less sensitive to probe the GC than detecting subhalos now. For the case of the Moore profile, sensitivity from GC observation is improved by 2 orders of magnitude, while only 1 order of magnitude improvement comes from subhalo observation. This means similar sensitivities will be achieved by observing the GC and subhalos.

On the contrary, subhalos provide a clean environment to search for the annihilation signals. Especially recent simulation shows that the DM profiles may not be universal. Smaller subhalos may have steeper central cusps [45,53]. Reed *et al.* gave the cusp index $\gamma = 1.4 - 0.08 \log(M/M_*)$ for halos of $0.01M_*$ to $1000M_*$ with a large scatter. In this case, if taking the GC the NFW profile and the subhalos the Moore profile, the γ-ray fluxes from the subhalos may even be greater than that from the GC.

I expect these sources can be detected by the satellite-based experiments, such as EGRET and GLAST. Once such sources are detected we can learn a lot about the nature of dark matter particles by studying its luminosity and spectrum of the annihilation. However, study shows that most of the EGRET unidentified γ-ray sources should not be of dark matter origin [6,23]. In this work I study how EGRET and GLAST can constrain the SUSY models if none of the subhalo γ-ray sources are detected in the two experiments.

I first realize 100 MW-like halos with subhalos whose distribution is given according to the N-body simulation results. In each realization I calculate the γ-ray flux from the subhalos by fixing the particle factor. Then I give the average cumulative number of the subhalo γ-ray sources as function of their flux intensities. Once the sensitivity of detectors, such EGRET and GLAST, are known, I know the detectable number of this kind of γ-ray sources. By requiring the detectable number smaller than 1 at EGRET and GLAST I put a constraint on the SUSY parameter space. My result shows that EGRET has already given a moderate constraint on the SUSY parameter space if I assume none of the unidentified γ-ray sources are from subhalos. GLAST can greatly enhance the constraints. However, a large uncertainty comes from the simulation, especially the property of subhalos in a dense environment. Convergence of the subhalos property in the future high resolution simulation will lead to more a precise constraint on the nature of dark matter particles.

[1] R. C. Hartman *et al.*, Astrophys. J. **123**, 79 (1999).

[2] G. Hobbs *et al.*, Mon. Not. R. Astron. Soc. **352**, 1439 (2004).

[3] J. M. Paredes, J. Marti, J. Ribo, and M. Massi, Mem. Soc. Astron. Ital. **73**, 900 (2002).

[4] D. F. Torres *et al.*, Phys. Rep. **382**, 303 (2003).

[5] S. J. Fegan *et al.*, Astrophys. J. **624**, 638 (2005).

[6] J. Flix, J. E. Taylor, M. Martinez, F. Prada, J. Silk, and J. Cortina, arXiv:astro-ph/0412419.

[7] G. Jungman, M. Kamionkowski, and K. Griest, Phys. Rep. **267**, 195 (1996).

[8] G. Belanger, F. Boudjema, S. Kraml, A. Pukhov, and A. Semenov, Phys. Rev. D **73**, 115007 (2006); A. Djouadi, M. Drees, and J.-L. Kneur, J. High Energy Phys. 03 (2006) 033; H. Baer, T. Krupovnickas, S. Profumo, and P. Ullio, J. High Energy Phys. 10 (2005) 020; H. Baer, A. Mustafayev, S. Profumo, A. Belyaev, and X. Tata, J. High Energy Phys. 07 (2005) 065; G. Belanger, S. Kraml, and A. Pukhov, Phys. Rev. D **72**, 015003 (2005); B. C. Allanach, G. Belanger, F. Boudjema, and A. Pukhov, J. High Energy Phys. 12 (2004) 020; J. Ellis, K. A. Olive, Y. Santoso, and V. C. Spanos, Phys. Lett. B **565**, 176 (2003).

[9] C. Munoz, Int. J. Mod. Phys. A **19**, 3093 (2004).

[10] J. L. Feng, K. T. Matchev, and F. Wilczek, Phys. Rev. D **63**, 045024 (2001); G. Bertone, D. Hooper, and J. Silk, Phys. Rep. **405**, 279 (2005).

[11] L. Bergstrom, P. Ullio, and J. Buckley, Astropart. Phys. **9**, 137 (1998); D. Horns, Phys. Lett. B **607**, 225 (2005).

[12] L. Bergström, J. Edsjö, P. Gondolo, and P. Ullio, Phys. Rev. D **59**, 043506 (1999); C. Calcaneo-Roldan and B. Moore, Phys. Rev. D **62**, 123005 (2000); A. Tasitsiomi and A. V. Olinto, Phys. Rev. D **66**, 083006 (2002); R. Aloisio, P. Blasi, and A. V. Olinto, Astrophys. J. **601**, 47 (2004); L. Pieri and E. Branchini, Phys. Rev. D **69**, 043512 (2004); N. W. Evans, F. Ferrer, and S. Sarkar, Phys. Rev. D **69**, 123501 (2004).

[13] S. M. Koushiappas, A. R. Zentner, and T. P. Walker, Phys. Rev. D **69**, 043501 (2004).

[14] X.-J. Bi, Y.-Q. Guo, H.-B. Hu, and X. Zhang, Nucl. Phys. **B775**, 143 (2007); Xiao-Jun Bi, Nucl. Phys. **B741**, 83 (2006).

[15] G. Tormen, A. Diaferio, and D. Syer, Mon. Not. R. Astron. Soc. **299**, 728 (1998).

[16] A. Klypin, S. Gottlöber, A. V. Kravtsov, and A. M. Khokhlov, Astrophys. J. **516**, 530 (1999); A. Klypin *et al.*, Astrophys. J. **522**, 82 (1999).

[17] B. Moore, S. Ghigna, F. Governato, G. Lake, T. Quinn, J. Stadel, and P. Tozzi, Astrophys. J. **524**, L19 (1999).

[18] S. Ghigna, B. Moore, F. Governato, G. Lake, T. Quinn, and J. Stadel, Astrophys. J. **544**, 616 (2000).

[19] V. Springel, S. D. M. White, G. Tormen, and G. Kauffmann, Mon. Not. R. Astron. Soc. **328**, 726 (2001).

[20] A. R. Zentner and J. S. Bullock, Astrophys. J. **598**, 49 (2003).

[21] G. De Lucia, G. Kauffmann, V. Springel, S. D. M. White, B. Lanzoni, F. Stoehr, G. Tormen, and N. Yoshida, Mon. Not. R. Astron. Soc. **348**, 333 (2004).

[22] A. V. Kravtsov, O. Y. Gnedin, and A. A. Klypin, Astrophys. J. **609**, 482 (2004).

[23] J. M. Siegal-Gaskins, V. Pavlidou, A. V. Olinto, C. Brown, and B. D. Fields, J. Phys. Conf. Ser. **60**, 312 (2007).

[24] A. Morselli, Int. J. Mod. Phys. A **17**, 1829 (2002).

[25] S. Peirani, R. Mohayaee, and J. A. de Freitas Pacheco, Phys. Rev. D **70**, 043503 (2004).

[26] S. M. Koushiappas, Phys. Rev. Lett. **97**, 191301 (2006).

[27] L. Pieri, G. Bertone, and E Branchini, arXiv:0706.2101v2.

[28] J. Conrad (GLAST-LAT Collaboration), arXiv:0706.0852.

[29] M. Kuhlen, J. Diemand, and P. Madau, AIP Conf. Proc. **921**, 135 (2007).

[30] G. Bertone, T. Bringmann, R. Rando, G. Busetto, and A. Morselli, astro-ph/0612387.

[31] E. A. Baltz, J. E. Taylor, and L. L. Wai, arXiv:astro-ph/0610731v2.

[32] J. Diemand, B. Moore, and J. Stadel, Mon. Not. R. Astron. Soc. **352**, 535 (2004).

[33] L. Gao, S. D. M. White, A. Jenkins, F. Stoehr, and V. Springel, Mon. Not. R. Astron. Soc. **355**, 819 (2004).

[34] J. Diemand, M. Kuhlen, and P. Madau, Astrophys. J. **657**, 262 (2007).

[35] F. Stoehr, S. D. M. White, V. Springle, G. Tormen, and N. Yoshida, Mon. Not. R. Astron. Soc. **345**, 1313 (2003).

[36] The physical cutoff of the minimal substructure is given in A. M. Green, S. Hofmann, and D. J. Schwarz, J. Cosmol. Astropart. Phys. 08 (2005) 003; Mon. Not. R. Astron. Soc. **353**, L23 (2004); S. Hofmann, D. J. Schwarz, and H. Stocker, Phys. Rev. D **64**, 083507 (2001).

[37] R. Aloisio, P. Blasi, and A. V. Olinto, Astrophys. J. **601**, 47 (2004).

[38] E. Hayashi, J. F. Navarro, J. E. Taylor, J. Stadel, and T. Quinn, Astrophys. J. **584**, 541 (2003).

[39] J. F. Navarro, C. S. Frenk, and S. D. M. White, Mon. Not. R. Astron. Soc. **275**, 56 (1995); Astrophys. J. **462**, 563 (1996); **490**, 493 (1997).

[40] A. Huss, B. Jain, and M. Steinmetz, Astrophys. J. **517**, 64 (1999); J. E. Taylor and J. F. Navarro, Astrophys. J. **563**, 483 (2001); A. Dekel, J. Devor, and G. Hetzroni, Mon. Not. R. Astron. Soc. **341**, 326 (2003); A. Dekel, I. Arad, J. Devor, and Y. Birnboim, Astrophys. J. **588**, 680 (2003); C. Power, J. F. Navarro, A. Jenkins, C. S. Frenk, S. D. M. White, V. Springel, J. Stadel, and T. Quinn, Mon. Not. R. Astron. Soc. **338**, 14 (2003).

[41] B. Moore, F. Governato, T. Quinn, J. Stadel, and G. Lake, Astrophys. J. **499**, L5 (1998); B. Moore, T. Quinn, F. Governato, J. Stadel, and G. Lake, Mon. Not. R. Astron. Soc. **310**, 1147 (1999).

[42] S. Ghigna, B. Moore, F. Governato, G. Lake, T. Quinn, and J. Stadel, Astrophys. J. **544**, 616 (2000); F. Governato, S. Ghigna, and B. Moore, arXiv:astro-ph/0105443; T. Fukushige and J. Makino, Astrophys. J. **557**, 533 (2001); **588**, 674 (2003).

[43] J. S. Bullock, T. S. Kolatt, Y. Sigad, R. S. Somerville, A. V. Kravtsov, A. A. Klypin, J. R. Primack, and A. Dekel, Mon. Not. R. Astron. Soc. **321**, 559 (2001).

[44] V. R. Eke, J. F. Navarro, and M. Steinmetz, Astrophys. J. **554**, 114 (2001).

[45] D. Reed, F. Governato, L. Verde, J. Gardner, T. Quinn, J. Stadel, D. Merritt, and G. Lake, Mon. Not. R. Astron. Soc. **357**, 82 (2005).

[46] A. Morselli, Int. J. Mod. Phys. A **17**, 1829 (2002).

[47] P. Gondolo, J. Edsjo, P. Ullio, L. Bergstrom, M. Schelke, and E. A. Baltz, J. Cosmol. Astropart. Phys. 07 (2004) 008.

[48] M. Kamionkowski, arXiv:0706.2986v1.

[49] R. Jeannerot, X. Zhang, and R. Brandenberger, J. High Energy Phys. 12 (1999) 003; W. B. Lin, D. H. Huang, X. Zhang, and R. Brandenberger, Phys. Rev. Lett. **86**, 954 (2001); M. Endo and F. Takahashi, Phys. Rev. D **74**, 063502 (2006); G. Gelmini, P. Gondolo, A. Soldatenko, and C. E. Yaguna, Phys. Rev. D **76**, 015010 (2007).

[50] P. Ullio, H. S. Zhao, and Marc Kamionkowski, Phys. Rev. D **64**, 043504 (2001).

[51] Gabrijela Zaharijas and Dan Hooper, Phys. Rev. D **73**, 103501 (2006).

[52] F. Aharonian *et al.* (H.E.S.S. Collaboration), Astron. Astrophys. **425**, L13 (2004).

[53] Y. P. Jing and Y. Suto, Astrophys. J. **529**, L69 (2000); **574**, 538 (2002).